

## PATCH CLAMP TECHNIQUES USED FOR STUDYING SYNAPTIC TRANSMISSION IN SLICES OF MAMMALIAN BRAIN

B. SAKMANN\*, F. EDWARDS\*, A. KONNERTH† AND T. TAKAHASHI‡

\* Max-Planck-Institut für medizinische Forschung, Abteilung Zellphysiologie, Heidelberg, FRG, † Max-Planck-Institut für biophysikalische Chemie, Göttingen, FRG and ‡ Department of Physiology, University of Kyoto, Japan

### SUMMARY

Procedures are described for recording postsynaptic currents from neurones in slices of rat brain using patch clamp techniques. The method involves cutting brain slices (120–300  $\mu\text{m}$  thick) with a vibrating microtome followed by localization of cell somata, which can be clearly seen with Nomarski differential interference contrast optics in the light microscope. Tissue covering the identified cell is then removed mechanically and standard patch clamp techniques are applied. Using these methods, spontaneously occurring and stimulus-evoked inhibitory postsynaptic currents (IPSCs) were recorded from neurones in rat hippocampus at greatly improved resolution. In the presence of tetrodotoxin, to block presynaptic action potentials, spontaneous IPSCs seldom exceeded 25 pA. Evoked IPSCs elicited by constant electrical stimulation of a presynaptic neurone were larger and fluctuated in their amplitudes. Single-channel currents, activated by the putative inhibitory transmitter  $\gamma$ -aminobutyric acid (GABA), had a size of about 1 pA. The number of postsynaptic channels activated by a packet of inhibitory transmitter is probably not more than thirty, nearly two orders of magnitude smaller than previously reported estimates for CNS synapses. This might reflect matching of synaptic efficacy to the high input resistance of hippocampal neurones and could be a requirement for fine tuning of inhibition.

### INTRODUCTION

Most of what is known about the functional characteristics of synaptic transmission and its underlying molecular constituents is derived from studies of peripheral synapses, most importantly the neuromuscular junction of skeletal muscle, the squid giant synapse (for review Katz, 1966) and the electromotor synapse of the electric ray *Torpedo* (for reviews Karlin, Cox, Kaldany, Lobel & Holtzman, 1983; Whittaker, 1984). At the neuromuscular synapse it was discovered that the release of acetylcholine from the presynaptic terminal is 'quantal' in nature (for review Katz, 1969) and that the postsynaptic action of acetylcholine is composed of many 'elementary' current events (Katz & Miledi, 1972). Estimates of the size and duration of the molecular components of the acetylcholine-activated postsynaptic current (Katz & Miledi, 1972; Anderson & Stevens, 1973; Neher & Sakmann, 1976) indicated that a packet of acetylcholine, when released from the nerve terminal, activated thousands of ion channels in the endplate. Much less is known about either the release of transmitter or the molecular components of postsynaptic transmitter action at synapses in the mammalian central nervous system (CNS) (for reviews Katz, 1969; Johnston & Brown, 1984). Postsynaptic currents at CNS synapses are much smaller than at peripheral synapses and conventional *in vivo* or brain slice preparations required the usage of high-resistance microelectrodes which limit current resolution. Furthermore, due to fact that neurones are covered by surrounding tissue and due to the complexity of synaptic connections in the

CNS, the precise neuronal type and the location of the synapse(s) studied are often not known. Mostly these technical limitations have prevented both the direct measurement of quantal components of postsynaptic currents in mammalian neurones and also the measurement of elementary events activated by the putative transmitter on a particular neurone.

Another, more quantitative way, to study synaptic transmission in the mammalian CNS would be to record from visually identified neurones in a particular brain area and stimulate a single presynaptic neurone. Patch clamp technique could then be used to achieve a higher resolution of the postsynaptic currents and to resolve elementary current events. Recently we have developed a preparation which allows the measurement of stimulus-evoked and spontaneous synaptic currents in identified neurones in the mammalian CNS, using the patch clamp technique (Edwards, Konnerth, Sakmann & Takahashi, 1989). This method involves the preparation of relatively thin slices (Takahashi, 1978) of brain tissue (120–300  $\mu\text{m}$  in thickness), followed by localized, visually controlled removal of neuropile covering the neuronal somata. Standard patch clamp techniques (Hamill, Marty, Neher, Sakmann & Sigworth, 1981) can then be applied to record evoked postsynaptic currents in almost any part of the brain, with a greatly improved current resolution. Single-channel currents can also be recorded from the same neurone. Here we illustrate the methods as applied to study inhibitory synapses in rat hippocampal neurones. The results indicate that the number of postsynaptic channels opened by a single packet of transmitter in hippocampal cells is surprisingly small, about two orders of magnitude smaller than at the neuromuscular junction or at other inhibitory CNS synapses.

## RESULTS

### *Preparation of thin slices of mammalian CNS*

The brain is removed quickly from rats of 18–23 days of age and is kept at low temperature (0–4 °C) in rat Ringer solution. Blocks of tissue 1–5 mm in thickness are mounted on the stage of a vibrating tissue slicer using a fast-drying glue (Cyanoacrylate, e.g. Uhu Sekundenkleber). Slices 120–300  $\mu\text{m}$  in thickness (Fig. 1*A*) are cut at high vibrating frequency (8–80 Hz). We used a Dosaka microslicer D.T.K.-1000 (Dosaka Co. Ltd, Kyoto, Japan) or an FTB Vibracut microtome (FTB, Weinheim, FRG).

Tissue slices are placed at room temperature in the experimental chamber, perfused with rat Ringer solution and held in place with a grid made from nylon threads on a metal frame (Fig. 1*B*). Slices of 120–150  $\mu\text{m}$  thickness allowed identification of individual neurones using a 40 $\times$  water immersion lens and Nomarski differential interference contrast optics (Takahashi, 1978). The outlines of many individual neurones can be seen easily by focusing through the thickness of the slice.

For electrophysiological recordings an upright microscope (Zeiss 'Standard') was modified such that the assembly of objective and oculars was moved during focusing while the slice and the pipettes remained stable (Fig. 2*A*). The table carrying the experimental chamber which contains the tissue slice (Fig. 2*B*) and the micromanipulators carrying the patch pipette and the cleaning or stimulating pipettes, were mounted together on a single block. They had no direct connection to the microscope, so that movements of the recording and stimulating pipettes relative to the slice were minimized during focusing.

A shortcoming of a water immersion lens is the difficulty of placing one or more pipettes correctly in the bath under the water immersion objective. To make this easier, a hinge was added to the backbone of the microscope (Fig. 2*A*). This modification allows a quick change

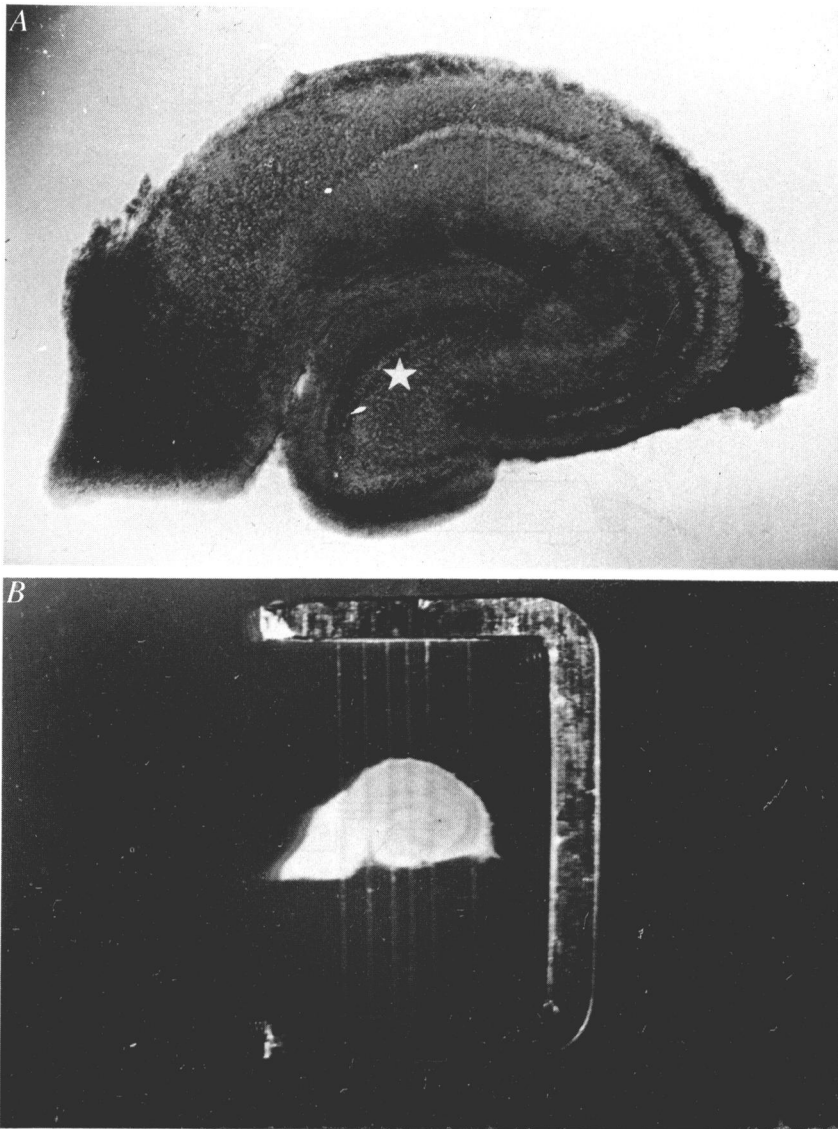


Fig. 1. Thin slices of rat brain. *A*, photomicrograph of thin slice of hippocampus as viewed with a dissecting microscope. The thickness of the slice is about  $150\ \mu\text{m}$ . CA1, CA2 and granular cell regions (star) are easily identified by their lighter appearance. *B*, stabilization of a slice for recording. Same slice as in *A*. Nylon threads glued to a metal frame hold the hippocampal slice on the bottom of the recording chamber. The dimensions of the grid are approximately  $7 \times 9\ \text{mm}$ .

of the recording or stimulating pipettes or of the slice, and the subsequent focusing onto the pipette tips under the water immersion lens is greatly simplified.

#### *Removal of neuropile from neuronal somata*

To allow access of the tip of the patch pipette to the neuronal membrane, the neuropile (glial and vascular tissue) overlying the nerve cell must be removed. Figure 3 shows schematically how this is achieved. Ringer solution is blown and sucked through a

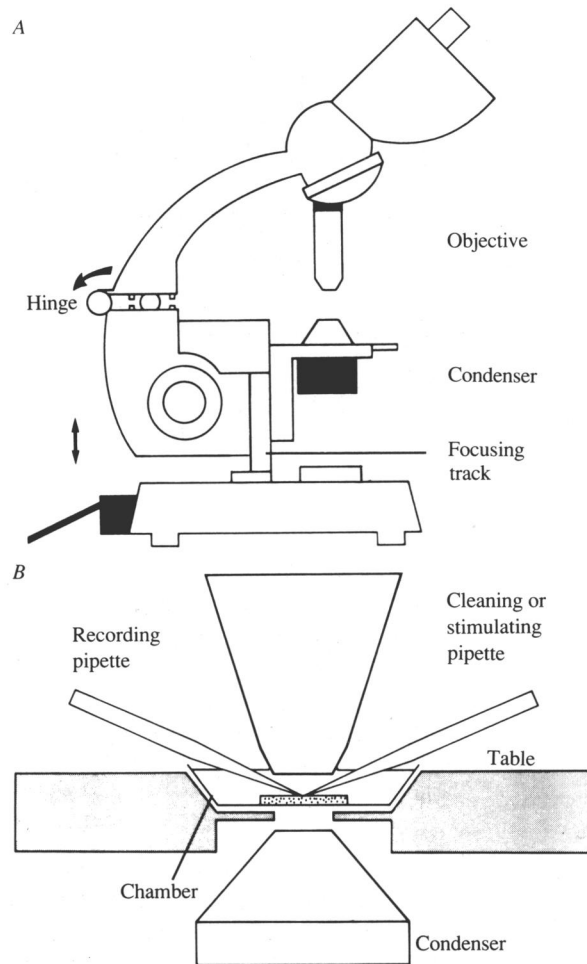


Fig. 2. Schematic drawing of experimental set-up. *A*, side view of modified Zeiss (Carl Zeiss, Oberkochen, FRG) 'Standard' microscope. The normal table of the microscope has been removed and is replaced by a modified table carrying the experimental chamber (not shown). This table is not attached to the microscope (not shown). the focusing track is attached to the base-plate. It moves the part carrying the oculars and the objective relative to the condenser and the table. A hinge allows removal of the objective during change of the pipettes and its return to the same position. *B*, detailed view of the arrangement of the water immersion objective, the recording chamber with slice (stippled) resting on the table as well as recording, cleaning or stimulating pipettes. They fit underneath the  $\times 40$  water immersion objective with a long (1.6 mm) working distance (objective 40/0.75 W, Carl Zeiss).

'cleaning' pipette which is placed with its tip directed at the immediate surroundings of the cell body of the neurone to be cleaned (Fig. 3 *A*). The cleaning pipette has a tip opening of 10–15  $\mu\text{m}$  and pressure and suction are delivered via the mouthpiece of a conventional patch pipette holder (Hamill *et al.* 1981). The jets of Ringer solution gradually break up the neuropile and eventually pieces of debris can be sucked away (Fig. 3 *B*).

Figure 4 shows photomicrographs of living cells after cleaning neurones in brain slices. In order to record from neurones with their dendritic trees as intact as possible, one chooses neurones lying about half-way into the depth of the slice. After removal of the overlying tissue the region under the pipette tip has a crater-like appearance when one focuses on the

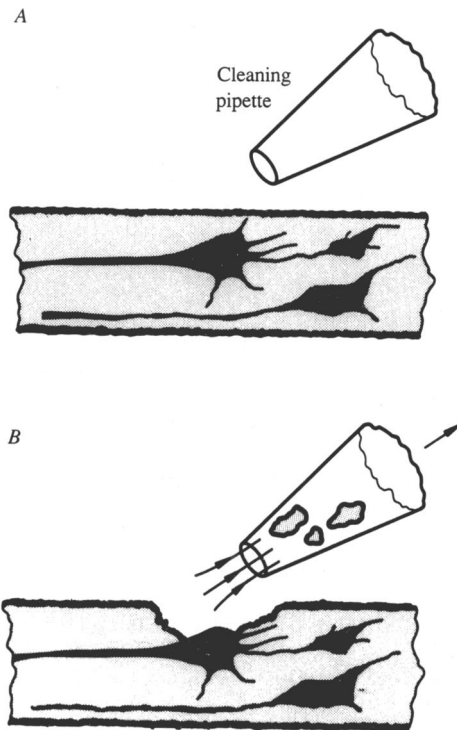


Fig. 3. Schematic drawing of localized cleaning of neuronal cell bodies. *A*, tip of cleaning pipette filled with Ringer solution is directed towards neuronal cell somata (in black) and jets of solution break up the overlying tissue (shaded). *B*, debris is sucked away into the tip of the pipette.

surface plane of the slice (Fig. 4*A*). The cleaned cell bodies of individual neurones lie at the bottom of the crater and are readily accessible to patch pipettes. This is shown in Fig. 4*B* for a group of pyramidal neurones in the CA1 layer of rat hippocampus.

In conventional slices (about 300–350  $\mu\text{m}$  in thickness; Alger, Dhanjal, Dingledine, Garthwaite, Henderson, King, Lipton, North, Schwartzkroin, Sears, Segal, Whittingham & Williams, 1984), neuronal somata can also be recognized and freed from overlying tissue in the same way as the neurones in thin slices (Fig. 4*C*). Identification of somata and cleaning is made much easier by the use of a standard video screen to observe the outlines of neurones to be cleaned and to monitor the removal of tissue. The use of these somewhat thicker brain slices improves the chance of recording from neurones with intact dendritic trees and this preparation is now used routinely in studies on hippocampal neurones.

#### *Inhibitory postsynaptic currents*

After forming a high-resistance seal on a hippocampal granule cell and breaking the membrane under the tip to establish the whole-cell recording configuration (Fig. 5*A*), spontaneously occurring currents of varying amplitude ( $< 10$ –200 pA, at  $-50$  mV) are always observed. These currents are reversibly blocked by bicuculline (2  $\mu\text{M}$ ) and reverse at the  $\text{Cl}^-$  reversal potential. They have thus been identified as  $\gamma$ -aminobutyric acid ( $\text{GABA}_\text{A}$ )-receptor-mediated inhibitory postsynaptic currents (IPSCs). In the presence of the  $\text{Na}^+$  channel blocker tetrodotoxin (TTX, 1  $\mu\text{M}$ ), the larger currents disappear and the remaining currents range in amplitude up to about 40 pA (Fig. 5*B*), with the vast majority of currents



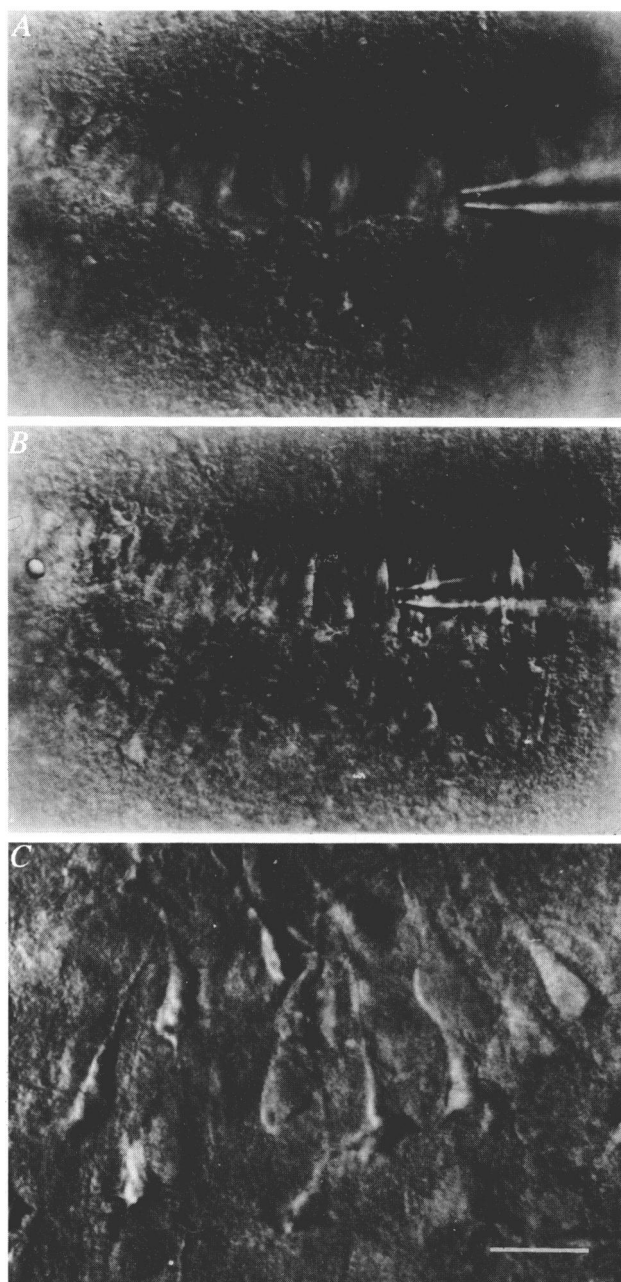


Fig. 4. Photomicrographs of living slices with exposed neuronal cell bodies. *A*, CA1 layer of rat hippocampus in a thin slice (about  $120\ \mu\text{m}$  in thickness). The plane of focus is the surface of the slice. Removal of tissue created a crater-like appearance in the slice. The tip of the cleaning pipette is seen on the right. *B*, same area of the slice but the plane of focus was changed to the neuronal cell bodies which are lying in the depth of a crater. Scale bar in the lower right corner is  $20\ \mu\text{m}$  for both *A* and *B*. *C*, photomicrograph of a cleaned area in rat CA1 hippocampal region in a conventional slice. The slice was cut to a thickness of about  $300\ \mu\text{m}$ . The neuronal somata were localized using a Kappa CF6 video camera (Kappa Messtechnik, Gleichen, FRG) attached to the microscope. The somata of pyramidal neurones are in the plane of focus. Scale bar is  $14\ \mu\text{m}$ .

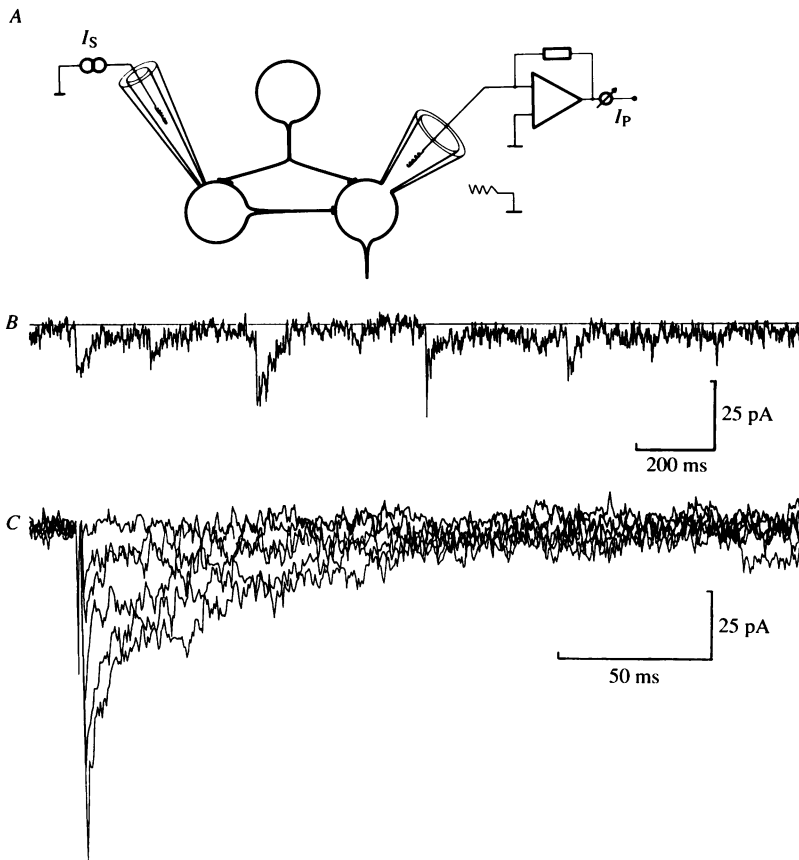


Fig. 5. Spontaneous and evoked IPSCs in granule cells of rat hippocampus. *A*, schematic drawing illustrating recording and stimulation via patch pipettes. IPSCs are recorded in the whole-cell recording configuration via a recording patch pipette ( $I_p$ ). Evoked IPSCs are elicited by stimulating a neighbouring neurone via an extracellular patch pipette ( $I_s$ ) with its tip placed onto the cell body of a neighbouring neurone. Direct depolarization of the neurone as well as depolarization of the nerve ending of another neurone close to the stimulating pipette might lead to stimulation of several synaptic inputs in the cell being recorded. *B*, records of spontaneous IPSCs in a granule cell. Whole-cell recording configuration. Membrane potential  $-50$  mV.  $1 \mu\text{M}$ -TTX was added to the bath solution to block action potentials invading presynaptic terminals. *C*, superimposed records of evoked unitary IPSCs elicited by electrical stimulation of a neighbouring neurone in a granule cell at  $-50$  mV. Evoked IPSCs are preceded by a stimulus artifact. The peak amplitude of IPSCs evoked by identical stimuli fluctuates between different levels which are approximately  $20$  pA apart. Records shown in *B* and *C* were filtered at  $2$  kHz low pass and digitized at  $5$  kHz. Composition of the bath solution (in mM): NaCl,  $125$ ; KCl,  $2.5$ ;  $\text{NaHCO}_3$ ,  $26$ ;  $\text{NaH}_2\text{PO}_4$ ,  $1.25$ ;  $\text{MgCl}_2$ ,  $1$ ;  $\text{CaCl}_2$ ,  $2$ ; glucose,  $25$  (pH  $7.4$ ), bubbled with  $95\%$   $\text{O}_2$  and  $5\%$   $\text{CO}_2$ . The pipette solution contained (in mM): *N*-methylglucamine,  $140$ ; HCl,  $125$ ;  $\text{CaCl}_2$ ,  $2$ ;  $\text{MgCl}_2$ ,  $1$ ; EGTA,  $10$ ; ATP,  $2$ ; HEPES,  $10$  (pH  $7.3$ ).

having amplitudes of less than  $25$  pA. They cannot be blocked by replacing  $\text{Ca}^{2+}$  by  $\text{Mg}^{2+}$  in the extracellular solution. These currents presumably result from spontaneous release (i.e. in the absence of presynaptic action potentials) of packets of transmitter from the inhibitory presynaptic terminal and are referred to as 'spontaneous' IPSCs.

To evoke a postsynaptic current by stimulating a presynaptic neurone, the tip of a patch pipette filled with rat Ringer solution is placed onto the soma of a partially cleaned neurone in the neighbourhood of the recorded neurone and short ( $200 \mu\text{s}$ ) voltage pulses ( $2$ – $10$  V) are applied to the pipette (Fig. 5*A*). Currents evoked in this way are characterized by short

delays ( $< 1$  ms) and brief ( $< 1$  ms) rise times. They always fluctuate in their amplitudes (Fig. 5C). Their decay time course has several components and has similar characteristics to the spontaneous IPSCs. These evoked currents are also blocked by bicuculline ( $2 \mu\text{M}$ ) and reverse at the  $\text{Cl}^-$  reversal potential. They have thus been identified as evoked IPSCs. In the presence of TTX ( $0.1 \mu\text{M}$ ), no currents are seen in response to stimulation. Thus they are shown to be due to stimulation of propagated action potentials in a presynaptic neurone and not due to local depolarization of presynaptic nerve terminals.

Extracellular stimulation sometimes results in activation of several synaptic inputs, as judged by differences in latencies of evoked IPSCs and by different stimulation thresholds of IPSCs. This may be due to depolarization of not only the soma of the cell on which the electrode is placed, but also of terminals of other neurones which innervate this cell body. Thus action potentials could be propagated in more than one cell resulting in release from two or more synapses (Fig. 5A). Initial attempts to record in the whole-cell configuration from two neighbouring neurones and elicit action potentials in only a single presynaptic neurone were successful, but the number of coupled cells was too low to use double whole-cell recording as a standard procedure. However, by adjusting the position of the stimulating pipette such that all evoked IPSCs are of similar latency and rise time, it seems likely that with extracellular stimulation action potentials can be elicited in a single presynaptic neurone and that the evoked currents (Fig. 5C) are 'unitary' evoked IPSCs (Faber & Korn, 1982) which represent the combined input from the active synaptic boutons of a single presynaptic neurone.

#### *Single-channel currents*

In order to estimate the number of channels activated during the peak of spontaneous IPSCs, which presumably reflects the release of a packet of transmitter, we measured single-channel currents in outside-out patches isolated from neuronal cell bodies. The measurements were made under similar conditions to the whole-cell recordings of IPSCs evoked by release of transmitter from the terminal. Figure 6A shows recordings of currents activated by GABA, the putative transmitter at these inhibitory synapses (Curtis, Felix & McLennan, 1970). The patch was isolated from the soma membrane of a granule cell of rat hippocampus. Amplitude distributions of such recordings indicate that at least two classes of elementary currents are activated, presumably reflecting different subtypes of  $\text{GABA}_\text{A}$  receptor channels with conductances of 14 and 23 pS. The number of channels activated during spontaneous IPSCs recorded from the same cell (Fig. 6B) thus is in the order of 15–25 channels assuming that the transmitter and GABA activate the same class of channels. The average decay time constant of spontaneous and unitary evoked IPSCs is comparable to the average duration of the GABA-activated elementary currents which would support the above assumption.

#### *Identification of neuronal cell types*

Confocal laser scanning microscopy (Åslund, Liljeborg, Forsgren & Wahlsten, 1987) in conjunction with loading cells with fluorescent dyes (e.g. Lucifer Yellow or Texas Red) is a convenient method to characterize in more detail the type of neurone from which a recording is made and to ensure the integrity of its dendritic tree (Wallén, Carlsson, Liljeborg & Grillner, 1988). Figure 7A shows the superposition of several scans taken at different levels of focus in the rat hippocampal granule cell from which IPSCs were recorded. A partial three-dimensional reconstruction of the dendritic tree of the same cell is shown in Fig. 7B. The cell was filled, via the patch pipette, with Lucifer Yellow, fixed



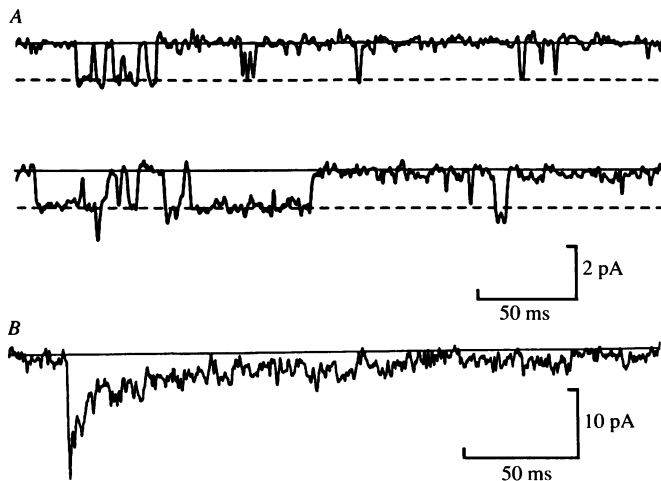


Fig. 6. Elementary currents activated by the putative transmitter GABA in granule cells. *A*, records of single-channel currents evoked by GABA application to an outside-out patch isolated from a hippocampal granule cell. Membrane potential  $-50$  mV. Solutions as described in Fig. 5. Baseline is indicated by continuous line. The dashed line indicates one open state of the GABA<sub>A</sub> receptor channel. *B*, for comparison, a spontaneous IPSC recorded from granule cell under similar ionic conditions and at  $-50$  mV membrane potential. Continuous line indicates baseline.

briefly, then scanned and reconstructed. Such reconstructions showed that the cell bodies of granule cells are small ( $10\text{--}15\text{ }\mu\text{m}$  in diameter) and that the dendritic processes of granular cells are extremely thin ( $< 3\text{ }\mu\text{m}$  in diameter at the widest points). The small size of their somata and their thin processes could account for the high input resistance (several gigohms) and low capacitance of these cells. To map the anatomical structure of the synaptic connections between cells from which a synaptic connection has been recorded one can fill the two neurones with different dyes (Edwards *et al.* 1989) then scan both neurones at different wavelengths, and determine the location of the contact zones between the pre- and postsynaptic neurones.

#### DISCUSSION

Patch clamp techniques used to record synaptic currents from visually identified neurones in brain slices allow the resolution of whole-cell current amplitudes as small as 8 pA whereas conventional single-electrode voltage clamp methods allowed resolution of about 100 pA (Edwards & Gage, 1988). This higher resolution made it possible to measure the amplitudes of spontaneous IPSCs and to demonstrate fluctuations in the amplitude of evoked unitary IPSCs elicited by constant electrical stimulation of a presynaptic neurone. The fluctuations of unitary IPSCs are roughly of the same size as the peak in the distribution of spontaneous IPSCs. This could suggest that evoked release is quantal in nature with a quantal conductance increase of  $0.2\text{--}0.4$  nS, considerably smaller than estimates ( $5\text{--}8$  nS) derived from the quantal analysis of inhibitory synaptic potentials in motoneurones (Kuno & Weakly, 1972). In goldfish CNS quantal conductance changes of tens of nS were derived (Faber & Korn, 1982; Korn, Mallet, Triller & Faber, 1982). These estimates were based solely on the analysis of fluctuations of evoked unitary IPSCs. In lamprey inhibitory synapses the size of spontaneous IPSCs also indicated quantal conductance changes in the range of tens of nS (Gold & Martin, 1983), but evoked unitary

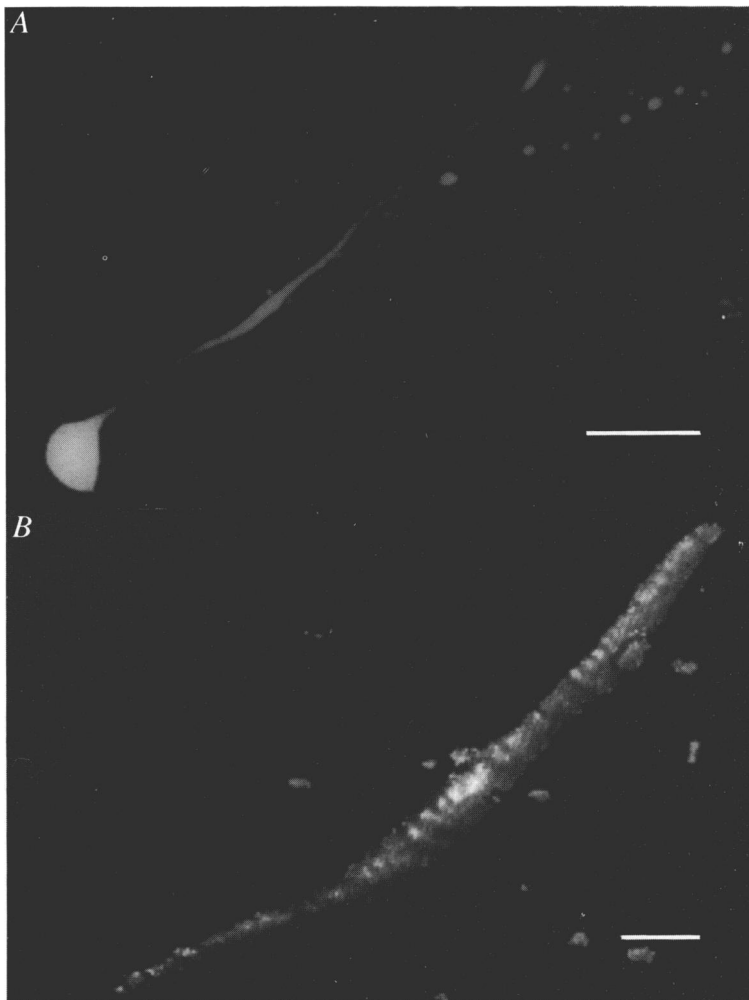


Fig. 7. Photomicrograph of computer-based reconstructions of rat hippocampal granule cell IPSCs were recorded in this cell in the granular cell layer of rat hippocampus using a patch pipette filled with the normal intracellular solution plus 1.5 mg/ml Lucifer Yellow (Sigma). After removing the patch pipette the slice was fixed for half an hour in paraformaldehyde, washed with phosphate buffer (pH 7.6) and then mounted in clearing solution of Moviol (Hoechst, Frankfurt, FRG) according to the recipe provided by Dr M. Osborn, M.P.I. für biphys. Chemie, Göttingen, FRG (Osborn, 1981). The cell was scanned through a Zeiss Axioskop built into the PHOIBOS confocal scanning system (Sarastro, Stockholm, Sweden). *A*, the cell was scanned using a  $\times 63$  oil immersion objective giving a resolution (pixel size) of  $0.2\ \mu\text{m}$ . Scans were made in eight planes with vertical intervals of  $0.2\ \mu\text{m}$  and added. This procedure allows two-dimensional visualization of the length of the cellular process although the cell does not lie exactly in the plane of the scanning. The scale bar represents  $15\ \mu\text{m}$ . *B*, three-dimensional reconstruction of the thicker section of the process of the cell shown in the upper panel, scanned at higher resolution. In the right half of the reconstruction the initial portions of two secondary dendrites can be seen. Note that the thinnest parts of the processes are lost by the (digital) filtering. The scans were made with  $\times 100$  oil immersion objective with a resolution (and pixel size) of  $0.13\ \mu\text{m}$ . Only one-sixteenth of the field shown in *A* was scanned. After taking repetitive scans (three per plane) in twenty planes at  $0.2\ \mu\text{m}$  intervals the sections were filtered, vectorized and then reconstructed. The scale bar represents  $5\ \mu\text{m}$ .

IPSCs could not be elicited. The small size of a quantal conductance change in hippocampal neurones reflects a much smaller number of postsynaptic channels activated during a quantal conductance change. Either a considerably smaller number of transmitter molecules is making up an axonally released packet or the number of postsynaptic receptor channels opposite a release site is rather smaller in hippocampal synapses. It has been suggested that in the CNS single synaptic boutons act as independent release units (Korn *et al.* 1982; Finkel & Redman, 1983; Gold & Martin, 1983). If the size of the quantal components of unitary IPSCs were limited by the number of available GABA receptors opposite a bouton then the weight of a particular synaptic knob could be drastically modified by inserting only a few additional receptors.

Thus far the morphological description of the CNS synapses studied functionally has not been possible. However, in conjunction with scanning confocal microscopy and image reconstruction, a rapid anatomical typing of the recorded neurone by its dendritic branching pattern and estimates of the number and location and the molecular constituents of physiologically identified synapses could be achieved. Future developments aimed at the functional characterization of synaptic transmission in the CNS using the techniques described here will be directed towards stimulation of a single presynaptic neurone via an intracellular microelectrode (Miles & Wong, 1984) and possibly changing its intracellular constituents. Under these conditions we can hope to achieve a similar degree of reproducibility as at the neuromuscular synapse and find out whether and how the rules governing synaptic transmission established at the neuromuscular junction by Bernard Katz and his school are to be modified at the rapidly transmitting synapses in the CNS.

Given the observation that long-term changes in inhibitory synaptic transmission in the hippocampus occur during postnatal development (Mueller, Taube & Schwartzkroin, 1984) and in adult animals in response to environmental stimuli (Edwards & Gage, 1988), the investigation of synaptic transmission by the techniques described here, in conjunction with the molecular characterization of GABA<sub>A</sub> receptor channel subtypes by cDNA techniques (Schofield, Darlison, Fujita, Burt, Stephenson, Rodriguez, Rhee, Ramachandran, Reale, Glencorse, Seeburg & Barnard, 1987; Pritchett, Sontheimer, Shivers, Ymer, Kettenmann, Schofield & Seeburg, 1989), might provide some insight into the pre- and postsynaptic mechanisms which govern long-term changes in the efficacy of inhibitory CNS synapses.

#### REFERENCES

- ALGER, B. E., DHANJAL, S. S., DINGLELINE, R., GARTHWAITE, J., HENDERSON, G., KING, G. L., LIPTON, P., NORTH, A., SCHWARTZKROIN, P. A., SEARS, T. A., SEGAL, M., WHITTINGHAM, T. S. & WILLIAMS, J. (1984). Brain slice methods. In *Brain Slices*, ed. DINGLELINE, R., pp. 381–437. New York: Plenum Press.
- ANDERSON, C. R. & STEVENS, C. F. (1973). Voltage clamp analysis of acetylcholine produced end-plate current fluctuations at frog neuromuscular junction. *Journal of Physiology* **235**, 655–691.
- ÅSLUND, N., LJLJEBORG, A., FORSGREN, P.-O. & WAHLSTEN, S. (1987). Three-dimensional digital microscopy using the PHOIBOS scanner. *Scanning* **9**, 227–235.
- CURTIS, D. R., FELIX, D. & McLENNAN, H. (1970). GABA and hippocampal inhibition. *British Journal of Pharmacology* **40**, 881–883.
- EDWARDS, F. A. & GAGE, P. W. (1988). Seasonal changes in inhibitory currents in rat hippocampus. *Neuroscience Letters* **84**, 266–270.
- EDWARDS, F. A., KONNERTH, A., SAKMANN, B. & TAKAHASHI, T. (1989). A thin slice preparation for patch clamp recordings from neurones of the mammalian central nervous system. *Pflügers Archiv* **414**, 600–612.

- FABER, D. S. & KORN, H. (1982). Transmission at a central inhibitory synapse. I. Magnitude of unitary postsynaptic conductance change and kinetics of channel activation. *Journal of Neurophysiology* **48**, 654–678.
- FINKEL, A. S. & REDMAN, S. J. (1983). The synaptic current evoked in cat spinal motoneurons by impulses in single group Ia axons. *Journal of Physiology* **342**, 615–632.
- GOLD, M. R. & MARTIN, A. R. (1983). Characteristics of inhibitory post-synaptic currents in brain-stem neurones of the lamprey. *Journal of Physiology* **342**, 85–98.
- HAMILL, O. P., MARTY, A., NEHER, E., SAKMANN, B. & SIGWORTH, F. J. (1981). Improved patch-clamp techniques for high-resolution current recording from cells and cell-free membrane patches. *Pflügers Archiv* **391**, 85–100.
- JOHNSTON, D. & BROWN, T. H. (1984). Biophysics and microphysiology of synaptic transmission in hippocampus. In *Brain Slices*, ed. DINGLEDINE, R., pp. 51–86. New York: Plenum Press.
- KARLIN, A., COX, R., KALDANY, R.-R., LOEBEL, P. & HOLTZMAN, E. (1983). The arrangement and functions of the chains of the acetylcholine receptor of *Torpedo* electric tissue. *Cold Spring Harbor Symposia on Quantitative Biology* **XLVIII**, 1–8.
- KATZ, B. (1966). *Nerve, Muscle and Synapse*. New York: McGraw Hill Book Company.
- KATZ, B. (1969). *The Release of Neural Transmitter Substances. The Sherrington Lectures X*. Liverpool: Liverpool University Press.
- KATZ, B. & MILEDI, R. (1972). The statistical nature of the acetylcholine potential and its molecular components. *Journal of Physiology* **224**, 665–699.
- KORN, H., MALLET, A., TRILLER, A. & FABER, D. H. (1982). Transmission at a central inhibitory synapse. II. Quantal description of release, with a physical correlate for binomial  $n$ . *Journal of Neurophysiology* **48**, 679–707.
- KUNO, M. & WEAKLY, J. N. (1972). Quantal components of the inhibitory synaptic potential in spinal motoneurons of the cat. *Journal of Physiology* **224**, 287–303.
- MILES, R. & WONG, R. K. S. (1984). Unitary inhibitory synaptic potentials in the guinea-pig hippocampus *in vitro*. *Journal of Physiology* **356**, 97–113.
- MUELLER, A. L., TAUBE, J. S. & SCHWARTZKROIN, P. A. (1984). Development of hyperpolarizing inhibitory postsynaptic potentials and hyperpolarizing response to  $\gamma$ -aminobutyric acid in rabbit hippocampus studied *in vitro*. *Journal of Neuroscience* **4**, 860–867.
- NEHER, E. & SAKMANN, B. (1976). Single-channel currents recorded from membrane of denervated frog muscle fibres. *Nature* **260**, 799–802.
- OSBORN, M. (1981). Techniques in cellular physiology – Part I. Localization of proteins by immunofluorescence techniques. *Techniques in the Life Sciences* **P107**, 1–28.
- PRITCHETT, D. B., SONTHEIMER, H., SHIVERS, B. D., YMER, S., KETTENMANN, H., SCHOFIELD, P. R. & SEEBURG, P. H. (1989). Importance of a novel GABA<sub>A</sub> receptor subunit for benzodiazepine pharmacology. *Nature* **338**, 582–585.
- SCHOFIELD, P. R., DARLISON, M. G., FUJITA, N., BURT, D. R., STEPHENSON, F. A., RODRIGUEZ, H., RHEE, L. M., RAMACHANDRAN, J., REALE, V., GLENCORSE, T. A., SEEBURG, P. H. & BARNARD, E. A. (1987). Sequence and functional expression of the GABA<sub>A</sub> receptor shows a ligand-gated receptor super-family. *Nature* **328**, 221–227.
- TAKAHASHI, T. (1978). Intracellular recording from visually identified motoneurons in rat spinal cord slices. *Proceedings of the Royal Society B* **202**, 417–421.
- WALLÉN, P., CARLSSON, K., LILJEBORG, A. & GRILLNER, S. (1988). Three-dimensional reconstruction of neurons in the lamprey spinal cord in whole-mount, using a confocal laser scanning microscope. *Journal of Neuroscience Methods* **24**, 91–100.
- WHITTAKER, V. P. (1984). The Synaptosome. In *Handbook of Neurochemistry*, vol. 7, 2nd edn, ed. LAJTHA, A., pp. 1–39. New York: Plenum Press.